

Thawing of the Active Layer on the Coastal Plain of the Alaskan Arctic

V. E. Romanovsky and T. E. Osterkamp

Geophysical Institute, University of Alaska, Fairbanks, AK 99775-7320, USA

ABSTRACT

Maximum active layer thicknesses increased from the coast inland with means of 0.36 m at West Dock, 0.53 m at Deadhorse, and 0.62 m at Franklin Bluffs and varied systematically from 1986 to 1992 by factors up to two (0.21 m to 0.45 m at West Dock). Maximum thicknesses occurred at all sites in 1989 and the recent data indicate a broad minimum from 1992 through 1995. Since trace gas emissions from tundra depend on active layer thicknesses, these results indicate potential systematic changes in trace gas emissions. A modified Kudryavtsev equation has advantages over other analytical models and accurately estimates active layer thicknesses in the Prudhoe Bay region. Stefan-type equations for predicting active layer thicknesses can lead to systematic errors of up to 71%. Temperatures at the ground surface when thawing ceases were estimated to be about 2 °C. The active layer typically reached its maximum thickness and began freezing upward from the bottom one to two weeks earlier than the beginning of freezing from the surface. Deviations (RMS) between calculated (using a calibrated finite element model) and measured temperatures were in the range 0.2–0.3 K indicating that a purely conductive heat flow model can be used for accurate predictions of active layer and permafrost temperatures. Previously estimated values of thermal offset were improved using adjusted thermal conductivity values indicated by the thermal modelling. © 1997 by John Wiley & Sons, Ltd.

RÉSUMÉ

L'épaisseur maximum de la couche active a augmenté depuis la côte avec des moyennes de 0.36 m à "West Dock", 0.53 m à "Deadhorse" et 0.62 m à "Franklin Bluffs" et a varié systématiquement de 1986 à 1992 selon des facteurs atteignant 2 (0.21 m à 0.45 m à "West Dock"). Les épaisseurs maximales ont été observées dans tous les sites en 1989 et les données récentes indiquent un large minimum de 1992 à 1995. Comme les émissions de gaz dépendent de l'épaisseur de la couche active, ces résultats indiquent un changement potentiel systématique dans l'émission des gaz. Une équation Kudryavtsev modifiée présente des avantages sur d'autres modèles analytiques et estime avec précision l'épaisseur de la couche active dans la région de Prudhoe Bay. Les équations de type Stefan pour prédire l'épaisseur de la couche active conduisent à des erreurs systématiques de plus de 71%. Les températures estimées à la surface du sol quand le dégel se termine, sont proches de 2 °C. La couche active atteint ordinairement son épaisseur maximum et commence à geler du fond vers le haut une à deux semaines plus tôt que le début du regel en surface. Des différences entre les températures calculées (en employant un modèle à éléments finis calibrés) et les températures mesurées sont de l'ordre de 0.2–0.3 K, indiquant ainsi qu'un modèle d'écoulement de la chaleur par seule conduction peut être utilisé pour prédire avec précision les températures de la couche active et du pergélisol. Des valeurs précédemment estimées des pertes thermiques ont été améliorées en utilisant des valeurs de conductivité thermique ajustées indiquées par le modèle thermique. © 1997 by John Wiley & Sons, Ltd.

Permafrost Periglac. Process., Vol. 8: 1–22 (1997).
(No. of Figs: 16. No. of Tables: 8. No. of Refs: 40)

KEY WORDS: active layer; permafrost; trace gases; modelling

INTRODUCTION

Air and ground temperature conditions, snow cover, and the active layer are important components for land–atmosphere interactions in the Arctic, and their investigation is one of the primary thrusts of Arctic system research. Permafrost occupies extensive areas in the Arctic. Northern ecological systems depend on permafrost conditions and permafrost directly influences human activities. At the same time, permafrost is extremely sensitive to climatic change. Therefore, studies of the interactions between permafrost and climate, especially during the period of possible climatic warming, are necessary parts of Arctic system research.

Permafrost is linked to the atmosphere by the intervening active layer, vegetation, and snow cover which vary strongly with time and location. It is important to develop a better understanding of the spatial and temporal behaviour of the active layer and upper permafrost to seasonal, annual, and multi-year changes in climate. Dynamics of the permafrost and active layer significantly influence the hydrology and hydrogeology of the land as well as its geomorphology. Together these conditions influence the biota and landscape so that permafrost and active layer dynamics plays a role in changes in the ecosystem as a whole.

Large amounts of carbon and methane are stored in permafrost below the annually thawed active layer which are not presently involved in the carbon cycle. Climatic warming may accelerate the rate of decomposition in the active layer, which is limited now by low temperatures, and thaw permafrost, making the organic soils available for decomposition. Some evidence already exists indicating that arctic tundra and boreal forests are changing from a carbon dioxide sink to a source (Kolchugina and Vinson, 1993; Oechel *et al.*, 1993; Oechel and Vourlitis, 1994). If there are strong temporal variations in active layer thicknesses, measurements of greenhouse gas fluxes may be time dependent.

Monitoring ground temperatures and active layer thicknesses and characteristics is also necessary for assessing changes in the environment (Barry *et al.*, 1994) which directly influence the conditions and quality of human life and activity in the circumpolar north. Active layer thicknesses are particularly important because of their direct effects on human activities, especially engineering features.

The interannual variability of the active layer thickness and the thermal regime of the active layer and near-surface permafrost were considered in previous publications (Romanovsky and Osterkamp, 1994; Romanovsky and Osterkamp, 1995a; Osterkamp and Romanovsky, 1996). This paper will concentrate on thermal processes in the active layer and near-surface permafrost during seasonal thawing, specifically how seasonal thawing progresses and methods for determining the maximum depth of the active layer. The data were obtained from 1986 to 1993 from high frequency (every four hours averaged daily) air, surface, active layer, and permafrost (down to 0.7–0.9 m) temperature measurements at three sites on the coastal plain of the Alaskan Arctic adjacent to the Beaufort Sea. The sites are along the Dalton Highway south from Prudhoe Bay and include West Dock (WD), Deadhorse (DH), and Franklin Bluffs (FB) (Figure 1). The data also include annually measured temperatures in the deeper boreholes (nominally 60 m) located at the same sites. Detailed descriptions of site conditions and methods of measurements and data processing have been published (Osterkamp, 1985; Osterkamp *et al.*, 1994; Romanovsky and Osterkamp, 1995a; Osterkamp and Romanovsky, 1996).

Approximate Analytical Solutions for the Thickness of the Active Layer

A number of simplified analytical solutions have been proposed to calculate active layer thicknesses (Lukyanov and Golovko, 1957; Porkhaev, 1970; Kudryavtsev *et al.*, 1974; Pavlov, 1980; Zarling, 1987; Balobaev, 1991; Aziz and Lunardini, 1992; 1993). One of the simplest is the Stefan equation

$$X = \sqrt{\left(\frac{2K_t I_t}{\rho L}\right)} \quad (1)$$

where X is the maximum thaw depth, K_t is the value of the soil thermal conductivity in the thawed state, I_t is the thawing index at the ground surface, ρ is the density, and L is the latent heat. The simplicity of the Stefan equation (1) is attractive and it has recently been used in a modified form (Hinkel and Nicholas, 1995)

$$X = b(\sqrt{I_t}) + a \quad (2)$$

where b is obvious from (1) and the intercept a was introduced to account for a non-zero intercept indicated by their data. Hinkel and Nicholas

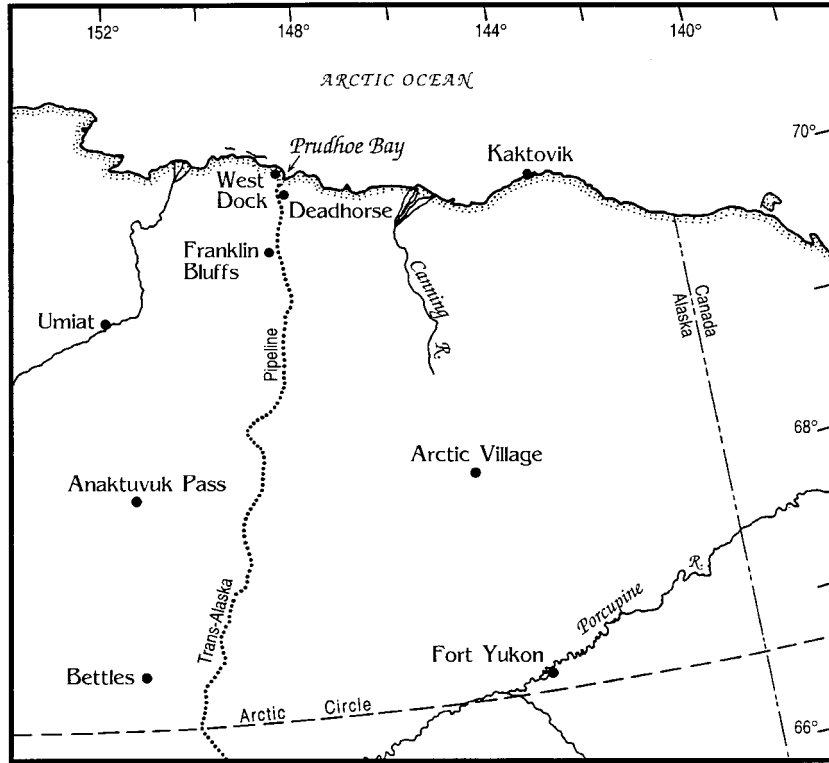


Figure 1 Map showing the study sites.

(1995) evaluated a and b by fitting two years of data on the partial thaw depths of an active layer with a very thick organic mat in a boreal forest setting underlain by discontinuous permafrost. Equation (2) does not appear to have been tested at other sites.

In deriving the Stefan equation, the assumption that the temperature in the frozen ground is equal to 0°C can produce significant errors in applications of this equation to regions of cold permafrost. The assumption of a small Stefan number, $C_t T / \rho L$, can also be restrictive in some cases. Temperature, T , is assumed to be a constant (it is not) during the period of thawing. This problem has been treated by using mean temperature values during thawing. However, it has been shown (Tipenko, 1987) that the function $X(t)$ depends not only on the value of the integral $\int_{t_0}^t T(t') dt'$, where t_0 is the time at the start of thawing, but also on the form of the surface temperature history $T(t)$. The spatial and temporal variations of the thermal properties of soils in the active layer also complicate the problem of predicting active layer depths for all models.

The Kudryavtsev equation (Kudryavtsev *et al.*, 1974)

$$X(2\bar{A}C_t + \rho L) = 2(A_{gs} - |\bar{T}_{ps}|) \sqrt{\frac{K_t C_t P}{\pi}} + (2\bar{A}C_t X_{2C} + \rho L X) \rho L \sqrt{\frac{K_t P}{\pi C_t}} \\ \frac{2\bar{A}C_t X_{2C} + \rho L X + (2\bar{A}C_t + \rho L) \sqrt{\frac{K_t P}{\pi C_t}}}{\pi} \quad (3)$$

with

$$\bar{A} = \frac{A_{gs} - |\bar{T}_{ps}|}{A_{gs} + \frac{\rho L}{2C_t}} - \frac{\rho L}{2C_t} \ln \frac{|\bar{T}_{ps}| + \frac{\rho L}{2C_t}}{\frac{\rho L}{2C_t}} \quad (4)$$

$$X_{2C} = \frac{2(A_{gs} - |\bar{T}_{ps}|) \sqrt{\left(\frac{K_t C_t P}{\pi}\right)}}{2\bar{A}C_t + \rho L} \quad (5)$$

where C_t is the thawed volumetric heat capacity, P is the period (one year), A_{gs} is the amplitude of annual periodic temperature variations at the ground surface and \bar{T}_{ps} is the mean annual permafrost surface temperature (MAPST), is much more complex. The necessary input data for this quadratic equation in X include averaged thermal properties of the active layer and \bar{T}_{ps} and A_{gs} . Equation (3) was derived with the assumption that there was no geothermal gradient and for a homogeneous active layer. For the area of investigations, a two-layered or even three-layered active layer is typical (Tables 1 and 5). Kudryavtsev proposed using this equation for calculating the maximum active layer thicknesses averaged over several years. Therefore, \bar{T}_{ps} and A_{gs} should be averaged over the same period. However, the calculations below show that (3) can be used on an annual basis.

Most of the equations for determining active layer thicknesses were derived with the assumption that the latent heat of phase change in the active layer is much larger than the sensible heat. Consequently, these equations are invalid as the latent heat approaches zero ($L \rightarrow 0$); however, the Kudryavtsev equation behaves differently. Substitution of $L = 0$ in (3), (4), and (5) yields

$$X = \sqrt{\left(\frac{K_t P}{\pi C_t}\right) \ln \frac{A_{gs}}{|\bar{T}_{ps}|}} \quad (6)$$

which is the equation for the maximum penetration depth of the 0°C isotherm in the case of a periodic steady state temperature regime in material without phase changes ($L = 0$) with harmonic temperature oscillations at the surface (where \bar{T}_{ps} is the mean annual temperature at the maximum depth of the 0°C isotherm which is also the amplitude at this depth).

Kudryavtsev's equation is a result of the application of the Fourier temperature wave propagation theory (see e.g. Tikhonov and Samarsky, 1966) to materials with phase changes ($L > 0$). It was derived with the assumption of a periodic steady state temperature regime (Kudryavtsev *et al.*, 1974). The equation can be simplified by introducing the dimensionless variables $\alpha = 2C_t A_{gs} / \rho L$ and $\beta = 2C_t |\bar{T}_{ps}| / \rho L$ which are analogous to the Stefan number (the ratio of sensible and latent heats) in the Neumann equation (e.g. Zarling, 1987). After some algebraic transformations, (3) becomes

$$X = X^* \sqrt{\left(\frac{K_t P}{\pi C_t}\right)} \quad (7)$$

Table 1 Soil type, dry bulk density and water content of the soils at the study sites (Romanovsky and Osterkamp, 1995a).

Depth (m)	Soil type	ρ_b kg m ⁻³	Gravimetric water content (%)	Volumetric water content (%)
<i>West Dock</i>				
0.0–0.10	Peat	—	319.3	—
0.10–0.20	Peat	455	150.0	68.2
0.20–0.31	Peat	371	207.1	76.8
<i>Deadhorse</i>				
0.0–0.12	Peat	—	119.0	—
1.12–0.23	Peat	531	113.0	60.0
0.23–0.40	Silt	1377	32.5	44.8
0.40–0.60	Silt	1250	36.0	45.0
<i>Franklin Bluffs</i>				
0.0–0.08	Peat	—	247.3	—
0.08–0.20	Peat	502	163.9	82.3
0.20–0.40	Silt	1466	34.0	49.8

where X^* is a solution to the quadratic equation

$$X^* \frac{\alpha - \beta}{\ln \frac{\alpha + 1}{\beta + 1}} = \alpha - \beta + \frac{X^* + \alpha - \beta - \ln \frac{\alpha + 1}{\beta + 1}}{X^* + \alpha - \beta - \ln \frac{\alpha + 1}{\beta + 1} + \frac{\alpha - \beta}{\ln \frac{\alpha + 1}{\beta + 1}}} \quad (8)$$

The variables α and β do not depend on K_t , making X^* independent of K_t also. Hence, (7) shows that the thickness of the active layer for the case of harmonic temperature oscillation at the ground surface is proportional to the square root of the thermal conductivity. The same is true for cases with step temperature changes at the ground surface (Stefan's equation and Neumann's solution).

A further advantage of (7) and (8) is that in (8) the solution for X^* depends only on two variables. This makes it possible to establish a simple nomogram (Figure 2) to estimate the value of X^* . The value of X^* can be also calculated from the solution to the quadratic equation (8)

$$X^* = B + \sqrt{(B^2 + D)} \quad (9a)$$

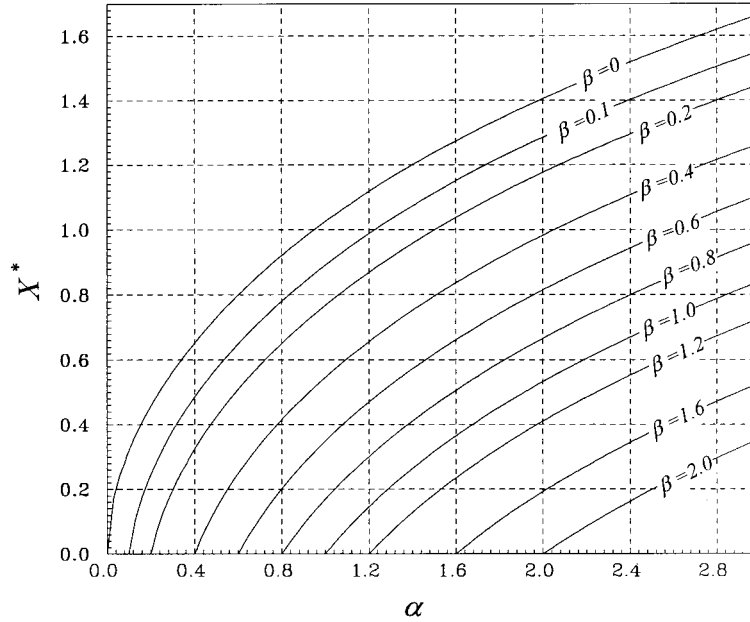


Figure 2 Nomogram for calculating the maximum annual thaw depth X . The dimensionless parameters are $\alpha = 2C_t A_{gs}/\rho L$ and $\beta = 2C_t |\bar{T}_{ps}|/\rho L$. X (m) should be calculated using the value of X^* from the nomogram and $X = X^* \sqrt{(D_t/\pi)}$, where D_t is the thermal diffusivity of the thawed soil ($\text{m}^2 \text{a}^{-1}$).

where

$$B = \delta + \frac{\delta}{2\gamma} - \frac{\gamma}{2\delta} - \frac{\gamma}{2} \quad (9b)$$

$$D = \delta + \delta\gamma + \gamma - \delta^2 - \frac{\delta^2}{\gamma} \quad (9c)$$

$$\gamma = \alpha + \beta \quad (9d)$$

$$\delta = \ln \frac{\alpha + 1}{\beta + 1} \quad (9e)$$

Equations (7) and (8) can be used to show another feature of the Kudryavtsev equation. Under the conditions which were used to derive (1) (\bar{T}_{ps} is equal to 0 and $L \rightarrow \infty$ with C_t constant), Kudryavtsev's equation (3) converts to Stefan's equation (1). Indeed, if $L \rightarrow \infty$, then $\alpha \rightarrow 0$, $\beta \rightarrow 0$, $\ln(\alpha + 1) \rightarrow \alpha$, and $\ln(\beta + 1) \rightarrow \beta = 0$, since $\bar{T}_{ps} = 0$. Substituting these values in (8), solving the quadratic equation, and taking only the lowest order of α (because $\alpha \rightarrow 0$) yields $X^* \cong \alpha^{1/2}$. Substitution of this result in (7) yields

$$X = \sqrt{\left(\frac{2K_t A_{gs} P}{\rho L \pi} \right)} \quad (10)$$

For harmonic oscillations with period P , mean temperature 0°C , and amplitude A_{gs} , the thaw

index becomes $I_t = (A_{gs} P)/\pi$ which makes equations (10) and (1) identical.

ANALYSIS AND DISCUSSION

Onset and Duration of Active Layer Thawing

The onset of thawing at the ground surface is closely related to snowmelt. Mean daily air temperatures during snowmelt typically varied around 0°C , but the ground surface temperatures must remain at or below 0°C until the snow melts completely. This is because the presence of both snow (ice) and water constrain the maximum surface temperature to the ice-point. Once the snow melts, the ground surface can warm above the ice-point and thawing of the active layer can begin. Dates for the beginning of thawing were taken to be the dates when the mean daily ground surface temperatures exceeded 0°C (Figures 3, 4 and 5). However, these are point measurements and may not represent the local tundra. The dates of snow disappearance (areal observations) at the Prudhoe Bay/ARCO station for 1987–92 are shown in Figure 6 together with dates for the beginning of the active layer thawing at WD, DH and FB sites

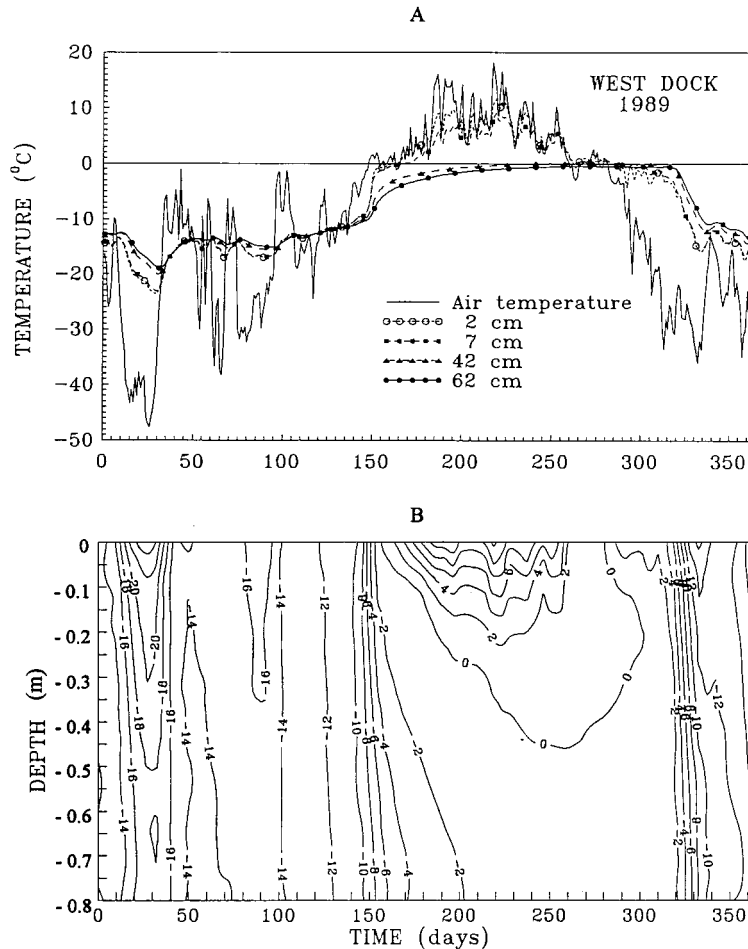


Figure 3 (A) Temperature–time series for different depths and (B) temperature field dynamics within the active layer and near-surface permafrost, at West Dock, Alaska, in 1989.

(see also Figures 3, 4, and 5). Given the limitations of the data, it is not possible to draw firm conclusions although some general trends seem evident.

At FB, ground thawing began about the same time or earlier than at WD and DH and usually preceded snowmelt at the ARCO station. This may be related to the typical pattern of snowmelt which begins earlier in the foothills compared with the coastal plain. Thawing started (Figure 6) uniformly at all sites between 4 June and 16 June during the first three years of measurements (except at FB in 1987). Average dates for the beginning of thawing were 9 June at WD, 6 June at DH, and 1 June at FB. Thawing started significantly earlier in 1990 (25 May for WD, 30 May for DH, and 17 May for FB), because of an extremely shallow snow cover during the 1989–90 winter and an anomalously

early snowmelt. At the Prudhoe Bay/ARCO meteorological station there was no snow during May 1990 and the maximum depth of snow during April was only 0.05 m. After 1990, the thawing dates were still earlier than 1987–89 for DH and FB (between 29 May and 1 June) and approximately the same for WD (12 June 1991 and 11 June 1992). There is a trend in Figure 6 toward earlier dates for the beginning of active layer thawing but the time series is relatively short. These data indicate that the beginning of thawing of the active layer depends primarily on factors that control the timing of snowmelt.

As air and ground surface temperatures increased, the active layer deepened progressively (Figures 3, 4, and 5). The rate of thawing was not uniform but increased during periods of warmer air and ground surface temperatures, and decreased

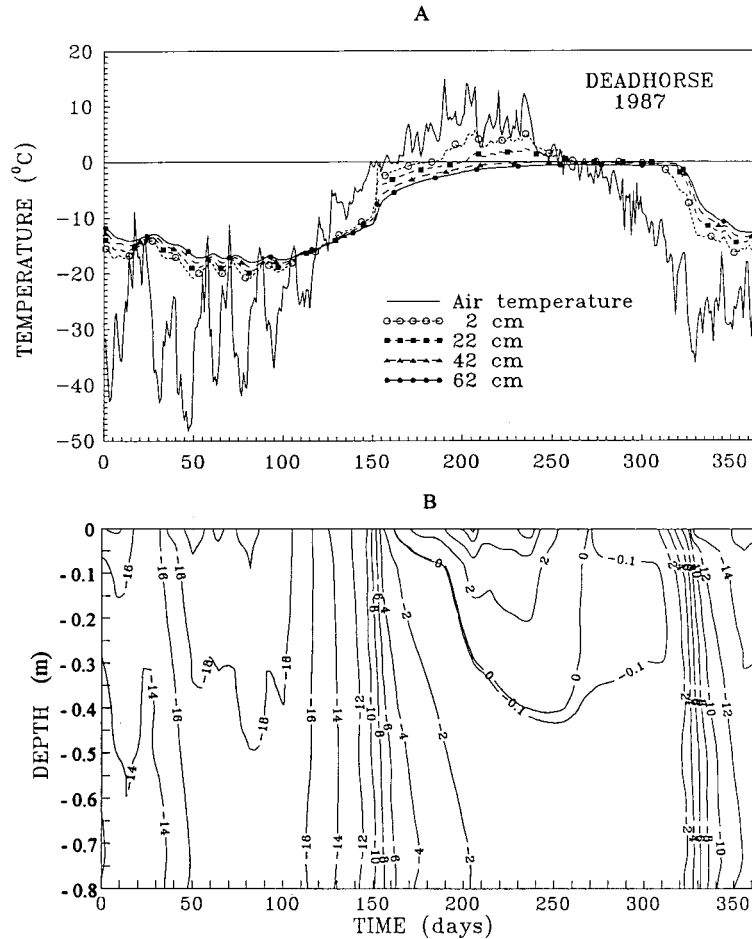


Figure 4 (A) Temperature–time series for different depths and (B) temperature field dynamics within the active layer and near-surface permafrost, at Deadhorse, Alaska, in 1987.

during stable and cooler periods. Some of these changes could be associated with changes in the active layer lithology and/or ice content in the soils.

Decreases in the thawing rate were measured, typically, within the lower 0.1–0.15 m of the active layer (Figures 3, 4, and 5) and are probably a result of changes in surface temperatures (which normally decrease in August) and decreases with time in the thawing rate even if surface temperature remains constant (Carslaw and Jaeger, 1959). However, they could also result from an increase in ice content near the base of the active layer due to upward freezing in the previous year (Shur, 1988).

A convenient approximation of the duration of the thaw season is the number of days with positive (above 0 °C) ground surface temperatures. However, the actual time of downward movement

of the thaw front is somewhat shorter. This can be seen from the requirement for energy conservation at the phase boundary

$$K_f G_f - K_t G_t = \rho L \frac{dX}{dt} \quad (11)$$

where K_f is the frozen thermal conductivity of the soil, and G_f and G_t are the frozen and thawed temperature gradients. The phase boundary velocity dX/dt becomes zero when

$$G_t = G_f K_f / K_t \quad (12)$$

For a linear temperature gradient in the thawed portion of the active layer, (12) is satisfied when the surface temperature is

$$T_s = G_f X K_f / K_t \quad (13)$$

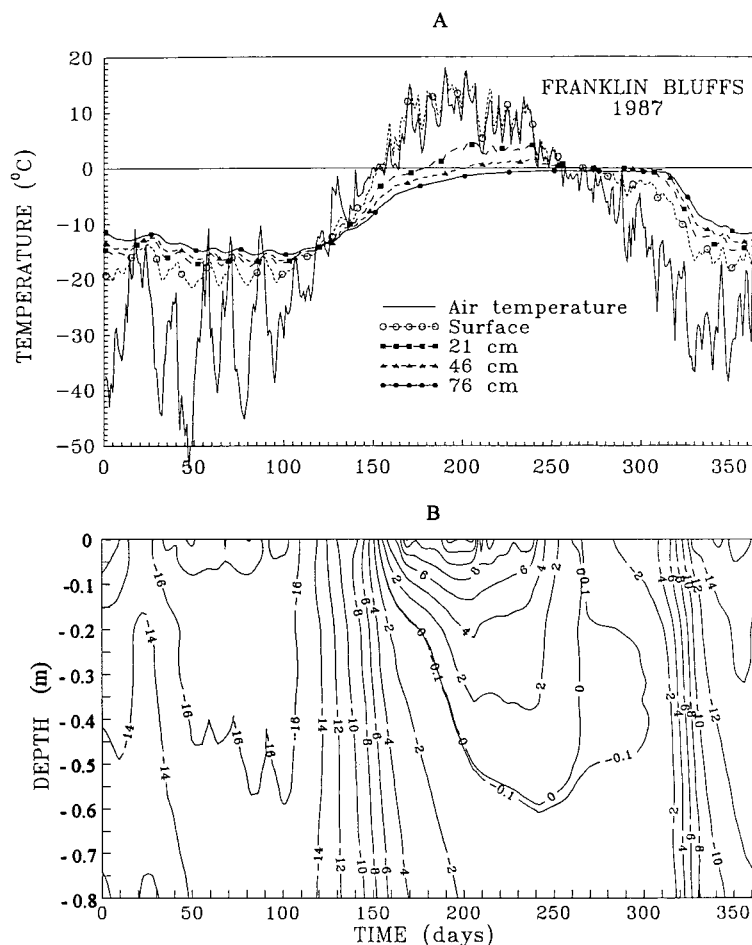


Figure 5 (A) Temperature–time series for different depths and (B) temperature field dynamics within the active layer and near-surface permafrost, at Franklin Bluffs, Alaska, in 1987.

Using the measured temperatures and estimated thermal conductivities for silt (Table 7), the values of T_s were calculated for each year for all three sites. Averaged over six years, the values were very similar for all sites: 1.75°C for WD and DH and, 1.9°C for FB. The ranges for T_s were also very similar: from 1.25°C to 2.8°C at WD, from 1.4°C to 2.2°C at DH, and from 1.6°C to 2.3°C at FB. Thus, when ground surface temperatures become colder than about +2°C the thawing season ends and the active layer begins freezing from the bottom upward.

At the WD, DH, and FB sites the active layer reached its maximum thickness and began freezing from the bottom upward about one to two weeks earlier than the beginning of freezing from the surface (Figures 3, 4, and 5). Figure 7 shows a comparison of these dates for all sites and for each

year. While average dates for the start of freezing from the surface were 16 September for WD, 18 September for DH, and 17 September for FB, average dates for maximum active layer thicknesses were 5 September for WD, 3 September for DH, and 4 September for FB.

Active Layer Thicknesses

Values of the mean annual ground surface temperature (MAGST) and A_{gs} together determine the value of I_t which influences the thickness of the active layer (Lachenbruch, 1959; Kudryavtsev *et al.*, 1974). The most important soil properties are the ice content which determines the value of latent heat, and the thermal conductivity and heat capacity in the frozen and thawed states (Kudryavtsev

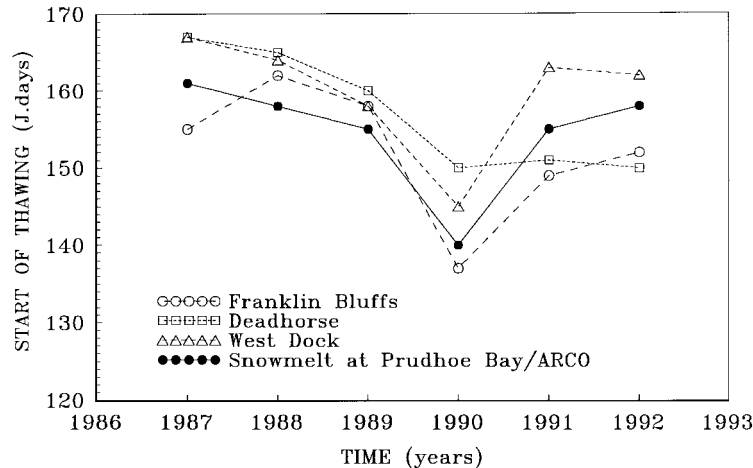


Figure 6 Interannual variations of the dates of snow disappearance at the Prudhoe Bay/ARCO station together with dates for the beginning of active layer thawing at West Dock, Deadhorse, and Franklin Bluffs.

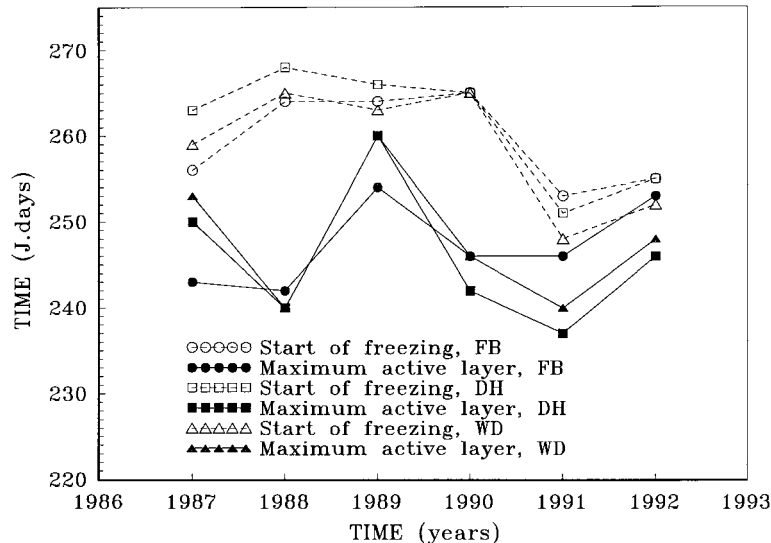


Figure 7. Interannual variations of the dates when the active layer reached its maximum thickness and dates for the start of the active layer refreezing from the ground surface downwards at West Dock, Deadhorse, and Franklin Bluffs.

et al., 1974; Pavlov, 1980; Balobaev, 1991). The value of \bar{T}_{ps} also influences the active layer thickness (Kudryavtsev *et al.*, 1974). In some cases (highly permeable soils), infiltration of summer precipitation can play a significant role in determining the thickness of the active layer (Kudryavtsev *et al.*, 1974). For the study area, this process probably did not have a noticeable effect on the active layer thickness because of the low water permeability of the soils and their saturated condition.

Active layer thicknesses increased from the coast inland with the increasing I_t and MAGST (Figure 8). The mean for measurements of the active layer thicknesses was 0.36 m at WD, 0.53 m at DH, and 0.62 m at FB. In general, variations in active layer thicknesses coincided with changes in MAGST and \bar{T}_{ps} , reaching a maximum in the warmest year (1989). However, the active layer thickness was more sensitive to summer temperatures (thawing index) (Figure 8B) than to MAGST (Figure 8A). Comparing 1990 and 1991 for FB and

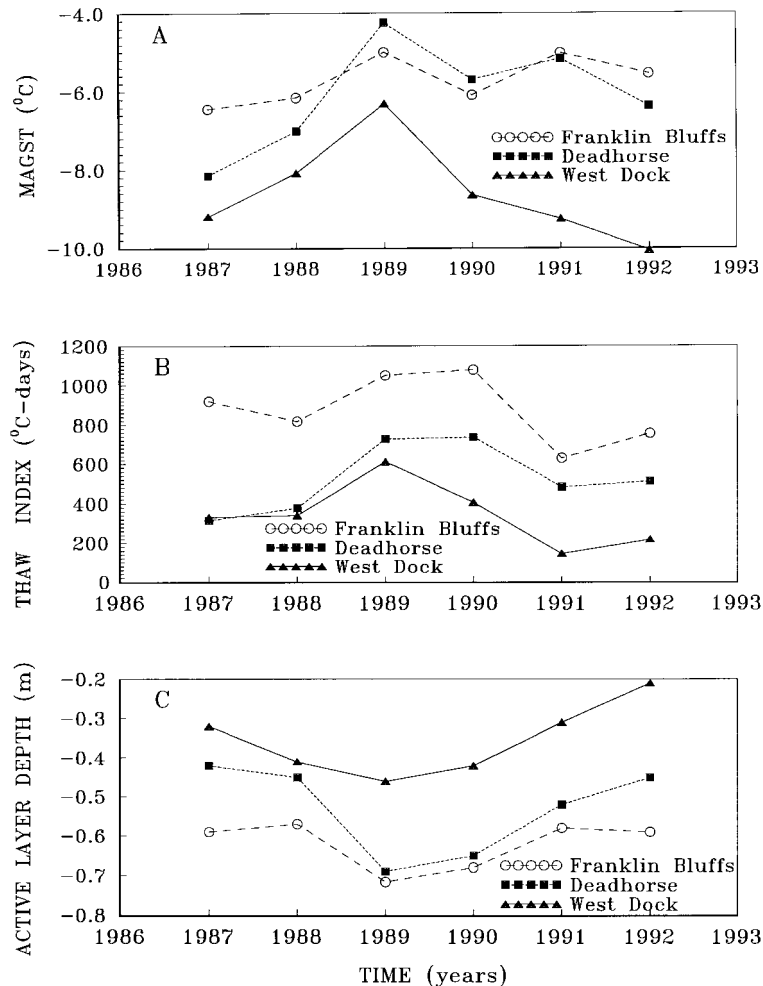


Figure 8 Temporal variations of (A) the mean annual ground surface temperatures, (B) the ground surface thaw index and (C) the active layer depth, for West Dock, Deadhorse, and Franklin Bluffs.

DH shows that the relative increase in MAGST in 1991 was due to a significantly warmer winter. The summer of 1991 was colder than 1990 and the thawing index in 1991 was 41% less for FB and 35% less for DH than in 1990 (Figure 8B). As a result, the active layer thickness in 1991 was 15% less for FB and 20% less for DH than in 1990 (Figure 8C). At FB, in spite of a decrease of MAGST from 1991 to 1992 (Figure 8A), the summer of 1992 was warmer and the thawing index was higher by 16% (Figure 8B). As a result, the active layer was slightly thicker by 2% (Figure 8C).

When the thawing index remained approximately constant, the MAGST and \bar{T}_{ps} became more important for the active layer thickness variations. The most typical years were 1987 and

1988, and 1991 and 1992, at DH and WD. While the thawing index remained almost constant (Figure 8B), the MAGST increased substantially from 1987 to 1988 (more than 1 °C) and decreased approximately by the same value from 1991 to 1992 (Figure 8A). As a result, the active layer thickness increased from 1987 to 1988 (by 7% for DH and 28% for WD) and decreased from 1991 to 1992 (by 14% for DH and 30% for WD) (Figure 8C).

Maximum active layer thicknesses have changed systematically from 1986 to 1992 (Figure 8C). At WD, they varied by a factor of two (from 0.21 m to 0.46 m) and at DH the range was similar (from 0.42 m to 0.69 m), while at FB it was about one-half that at WD and DH (from 0.57 m to 0.71 m). Maximum thicknesses occurred at all sites in 1989

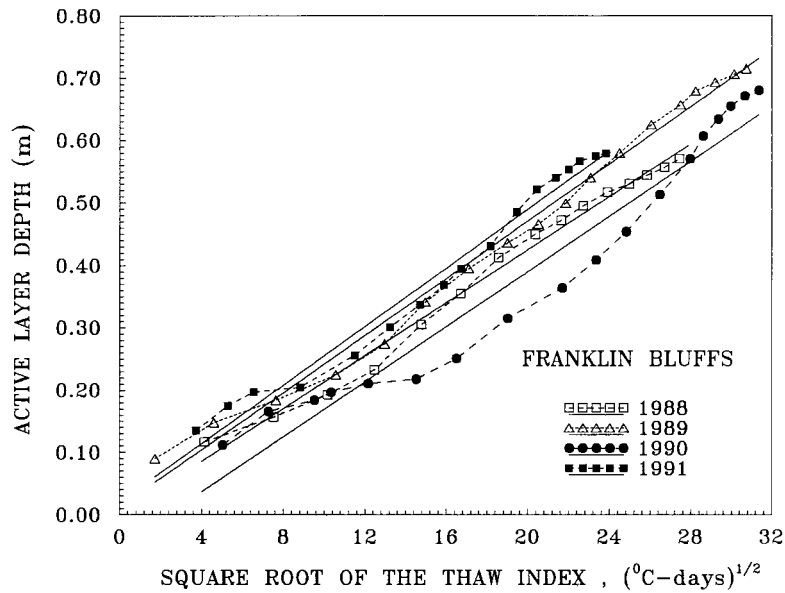


Figure 9 Relationship between the measured thaw depth and square root of thaw index at the ground surface for selected thaw seasons at Franklin Bluffs. Some seasons were omitted for clarity.

and recent data indicate a broad minimum from 1992 until 1995. Unfortunately, the data time series are not yet long enough to determine if these changes are part of natural variability, a cycle or a trend. These large interannual variations of active layer thicknesses make a comparative analysis of the spatial behaviour of the active layer difficult.

Since trace gas emissions from the tundra depend on temperatures, active layer thicknesses and water table levels among other factors, then these results suggest potential systematic changes in the emissions. Indeed the tundra appears to have recently changed from a sink to a source of CO_2 (Oechel *et al.*, 1993; Oechel and Vourlitis, 1994). If the observed changes in active layer thicknesses are part of a cycle then this would imply a reversal of their result in the near future. Thus, it is important to have a long-term record of ground temperatures and active layer thicknesses.

Figures 9, 10, and 11 show how thaw depth relates to the thaw index over the summer thawing period for WD, DH, and FB. These data show that the functional dependence of thaw depth changes not only from site to site, but also from year to year for each site. Some years show somewhat similar curves (1987 and 1988 for DH; 1988, 1989 and 1991 for FB) but significant differences are more common (all four curves for WD; 1992 and all other curves for DH; 1990 and all other curves for FB). Moreover, these curves change form during a

single year. This could be a result of changes in thermal properties of the soils with depth and/or time during the year (due to variations in lithology and/or water content).

The solid lines in Figures 9, 10, and 11 are a fit of (2) to the data for selected thaw seasons. At FB (Figure 9), the value for the slope b in (2) remains practically constant (2.12 to 2.34). However, differences in the intercept a exceed 0.1 m. At DH (Figure 10), values of the slope b vary from 2.28 to 2.92 and, at WD (Figure 11), b varies from 1.37 to 2.45. These variations in the parameters of (2) lead to maximum errors of 14%, 37%, and 51% at FB, DH, and WD, respectively. Consequently, it appears that (2) can be used with confidence only at FB and would lead to relatively large errors at the other sites.

The maximum active layer thicknesses were calculated using the Stefan equation (1) and modified Kudryavtsev equations (7)–(9) using the thermal properties in Table 2. All properties were averaged over the full thickness of the active layer using a series heat conduction model. Estimates of the thermal diffusivity of the active layer (Zhang, 1993) were used to calculate C_t . In the Kudryavtsev equation (3), A_{gs} is one-half of the annual range in the mean monthly temperatures at the ground surface averaged over several years. In these annual calculations, A_{gs} was estimated for each year as the difference between the MAGST and the warmest

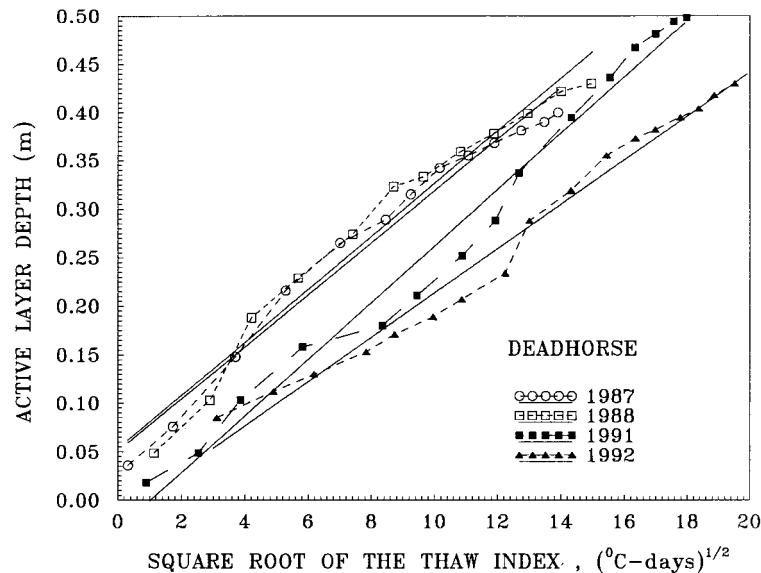


Figure 10 Relationship between the measured thaw depth and square root of thaw index at the ground surface for selected thaw seasons at Deadhorse. Some seasons were omitted for clarity.

monthly mean in the ground surface temperatures for the corresponding year.

The results of these calculations (Table 3) show that the Stefan equation overestimates the active layer depth probably because it does not take into account the heat flux into the permafrost at the permafrost table (in the case of cold permafrost this overestimation is significant). The maximum

average percentage difference between the measured and calculated values for Kudryavtsev's equation was -6% and the range of values was -38% to $+26\%$ while for Stefan's equation these values were $+26\%$, -3% , and $+71\%$.

To further examine the modified Kudryavtsev's equation (7–9), the results were compared with numerical calculations of the active layer

Table 2 Thermal properties of the active layer used in the calculations with equations (1) and (7–9).

Site	Average volumetric water content θ (%)	Average latent heat ρL (MJ m^{-3})	Thermal conductivity K_t ($\text{W m}^{-1}\text{K}^{-1}$)	Heat capacity C_t ($\text{MJ m}^{-3}\text{K}^{-1}$)
West Dock	72.5	242	0.60	2.70
Deadhorse	51.5	172	0.77	2.36
Franklin Bluffs	58.3	195	0.82	2.30

Table 3 Thicknesses of the active layer (m) calculated using the Stefan equation (Stef), modified Kudryavtsev equation (Kud), and measured (Meas) values.

Year	West Dock			Deadhorse			Franklin Bluffs		
	Stef	Kud	Meas	Stef	Kud	Meas	Stef	Kud	Meas
1987	0.46	0.34	0.32	0.49	0.36	0.42	0.82	0.63	0.59
1988	0.44	0.36	0.41	0.53	0.44	0.45	0.77	0.67	0.57
1989	0.59	0.49	0.46	0.79	0.74	0.69	0.87	0.75	0.71
1990	0.52	0.38	0.42	0.70	0.68	0.65	0.88	0.86	0.68
1991	0.30	0.19	0.31	0.62	0.54	0.52	0.68	0.53	0.58
1992	0.36	0.25	0.21	0.66	0.49	0.45	0.74	0.64	0.59
Mean	0.44	0.32	0.35	0.63	0.50	0.53	0.79	0.65	0.62

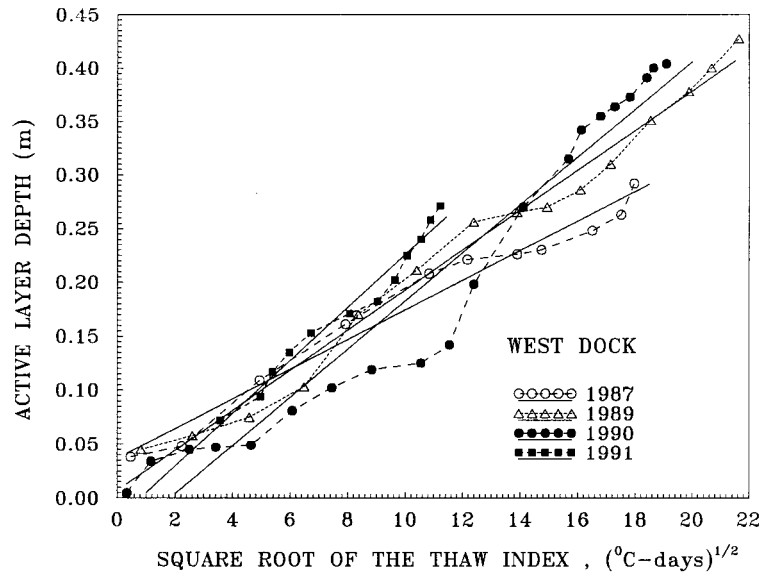


Figure 11 Relationship between the measured thaw depth and square root of thaw index at the ground surface for selected thaw seasons at West Dock. Some seasons were omitted for clarity.

thicknesses using a hypothetical periodic steady state surface temperature (Goodrich, 1976). The values of \bar{T}_{ps} and A_{gs} which were used in these calculations are shown in the first two columns of Table 4. The thermal properties used in these calculations were $K_t = 1.13 \text{ W m}^{-1} \text{ K}^{-1}$, $C_t = 3.15 \text{ MJ M}^{-3} \text{ K}^{-1}$, and $\rho L = 151.97 \text{ MJ m}^{-3}$. Comparison of these results for different temperature conditions at the ground and permafrost surface with results provided by equations (7) and (9) shows a maximum percentage difference of 9%.

Numerical Modelling of the Active Layer and Near-Surface Permafrost Temperature Regime During Seasonal Thawing

Figures 9 through 11 indicate that significant inter-annual changes may have occurred in the thermal properties of the soils (primarily in the thermal conductivity) especially at WD and DH. Numerical simulations of the active layer and near-surface permafrost temperature regime were used to examine this possibility and to evaluate the use of a purely conductive heat flow model with moving phase boundary to describe the temperature field dynamics for the case of seasonal thawing.

A finite element model (Gosink and Osterkamp, 1990; Osterkamp and Gosink, 1991; Osterkamp

Table 4 Comparison of calculations for active layer thicknesses obtained using a numerical method (Goodrich, 1976) and equations (7) and (9).

\bar{T}_{ps} (°C)	A_{gs} (K)	Active layer thickness (m)	
		Goodrich	Eqs (7) and (9)
2.67	15.00	1.40	1.29
-11.10	20.00	0.74	0.70
-4.50	11.10	0.84	0.77
-4.24	12.25	0.85	0.89
-8.14	14.85	0.76	0.69

and Romanovsky, 1996), which is a modified version of the Guymon and Hromadka (1977) and Guymon *et al.* (1984) model, was used to reconstruct the one-dimensional temperature field in the active layer and near-surface permafrost. Mean daily ground temperatures measured from 1986 to 1992 at the ground surface (0.02 m at WD and DH, and 0.0 m at FB) were used for the upper boundary conditions. The lower boundary was placed at the 16 m depth. Daily temperatures at this depth were calculated for all sites for the period of measurements (1987 through 1992) in the process of reconstructing the daily permafrost temperatures to the 60 m depth (Romanovsky and Osterkamp, 1995b; Osterkamp and Romanovsky, 1996). A combination of the daily temperature profiles measured to the depth of 0.7–0.8 m and calculated to the depth of 55 m from Osterkamp

Table 5 Thermal properties of the active layer and near-surface permafrost estimated from the results of previous investigations.

Depth (m)	Soil type	Volumetric water content θ (%)	Volumetric heat capacity C_t/C_f ($\text{MJ m}^{-3}\text{K}^{-1}$)	Thermal conductivity K_t/K_f ($\text{W m}^{-1}\text{K}^{-1}$)
<i>West Dock</i>				
0.0–0.2	Peat I	68.2	2.7/1.26	0.6/1.2
0.2–0.35	Peat II	76.8	2.7/1.26	0.6/1.2
0.35–0.9	Silt	44.4	2.1/1.54	1.2/1.56
0.9–8.5	Silt and sand	43.4	2.9/2.34	2.0/3.39
8.5–16	Sand and gravel	38.9	2.9/2.04	2.0/3.39
<i>Deadhorse</i>				
0.0–0.12	Peat I	–	2.7/1.26	0.6/1.2
0.12–0.23	Peat II	60.0	2.7/1.26	0.6/1.2
0.23–0.92	Silt	45.0	2.1/1.54	1.35/1.76
0.92–2.7	Sand and silt	–	– /2.14	– /3.39
2.7–16	Gravel	–	– /1.94	– /3.59
<i>Franklin Bluffs</i>				
0.0–0.08	Peat I	70.0	2.7/1.26	0.6/1.2
0.08–0.2	Peat II	80.3	2.7/1.26	0.6/1.2
0.2–1.2	Silt	48.0	2.1/1.54	1.35/1.76
1.2–14	Gravel	–	– /1.94	– /3.59
14–16	Silt	–	– /1.54	– /1.76

and Romanovsky (1996) were used for the initial conditions.

Drilling records were used to determine the lithology, and results of previous investigations (Lachenbruch *et al.*, 1982; Lachenbruch and Marshall, 1986; Hinzman *et al.*, 1991; Zhang, 1993; Romanovsky and Osterkamp, 1995a; Osterkamp and Romanovsky, 1996) were used to approximate the initial thermal properties of the soils in the thawed and frozen states (Table 5). The time step in these calculations was 1 hour, while the space steps (200) were changed from 0.01 within the upper 1 m of soils to 1 m at the lower boundary of the space domain (16 m).

The results of calculations for the WD site in 1987 using the finite element model were compared with a simulation using a one-dimensional finite difference model (Goodrich, 1976; 1978) with exactly the same input parameters and space steps. It was found that, for the case of small time steps (1 hour for the finite element model and 7 minutes for the finite difference model), the calculated daily temperatures from both models differed by only 0.02°C for the whole year (1987) for 18 selected output depths from 0.02 to 0.87 m (every 0.05 m), except for one day just after freeze-up, when the difference reached 0.35°C at the depth of 0.17 m. The RMS deviation between the results of these

two models for the whole year and for these 18 depths was 0.012°C .

It was impossible (especially for the WD and DH sites) to produce reasonably small deviations (less than $0.5\text{--}0.6^\circ\text{C}$) between measured and calculated values with the model using the same soil parameters for each year during the period from 1987 to 1992. Starting with the initial approximations for the thermal properties of the soils (Table 5) those values were adjusted each year, where necessary, by trial and error to produce the smallest differences between calculated and measured temperature profiles (Figures 12, 13, and 14). Only values of the thermal conductivity of soils in thawed and frozen states were changed, while heat capacity and latent heat were kept the same. With the thermal conductivity held constant during each year but allowed to change from year to year the deviations (RMS) between calculated and measured temperatures were in the range $0.2\text{--}0.3^\circ\text{C}$, except for an unexplained increase in 1990 at WD and in 1989 at FB (Table 6). The large value of the RMS deviations in 1989 at DH may be associated with the short interruption in data (Romanovsky and Osterkamp, 1995a) due to flooding of the site. A comparison between calculated and measured temperatures at several depths during 1987 and 1988 for the DH site

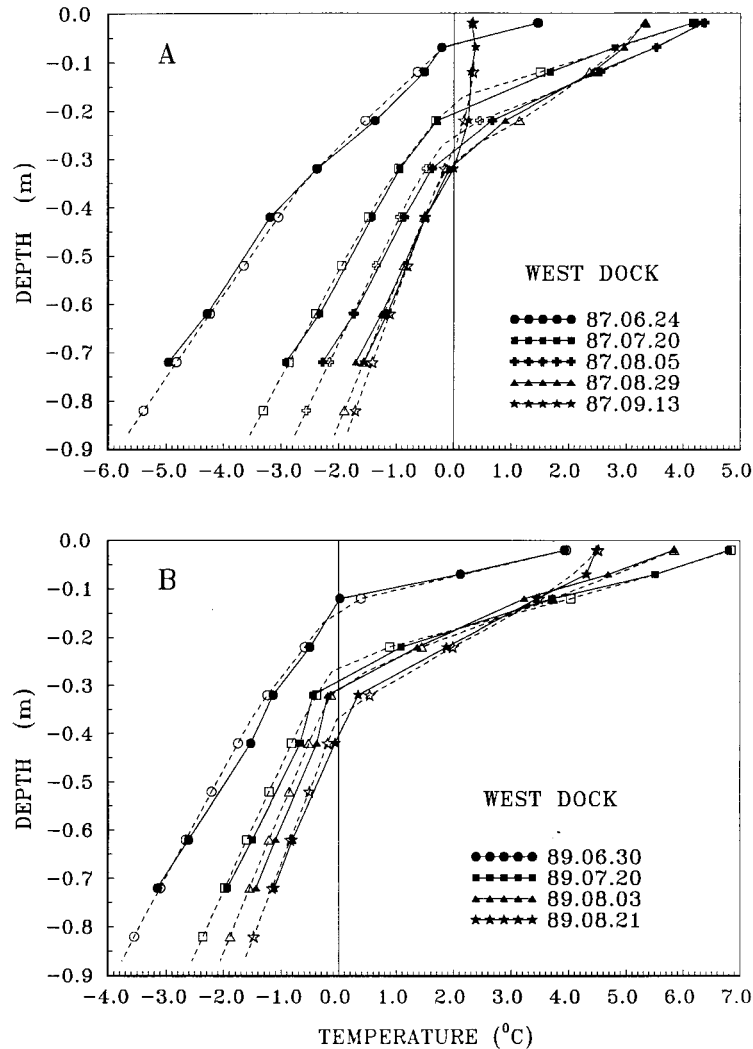


Figure 12 Calculated (dashed lines and open symbols) and measured (solid lines and filled symbols) temperature profiles at West Dock during the thawing period in 1987 and 1989.

(Figure 15) shows that the differences are very small. The differences were most pronounced during the period of warming and especially during the period of cooling after freeze-up when they can be explained by the influence of unfrozen

water in the partially frozen soils (Osterkamp and Romanovsky, 1997).

Examples of measured and calculated temperature profiles are shown in Figures 12, 13, and 14. The values of the thermal conductivities which

Table 6 Values of the root mean square deviations (RMS) of calculated mean daily temperatures from the measured ones.

Site	1987	1988	1989	1990	1991	1992	Average
West Dock	0.14	0.22	0.25	0.63	0.34	0.35	0.33
Deadhorse	0.24	0.21	0.68	0.31	0.32	0.25	0.34
Franklin Bluffs	0.31	0.20	0.59	0.24	0.17	0.22	0.29

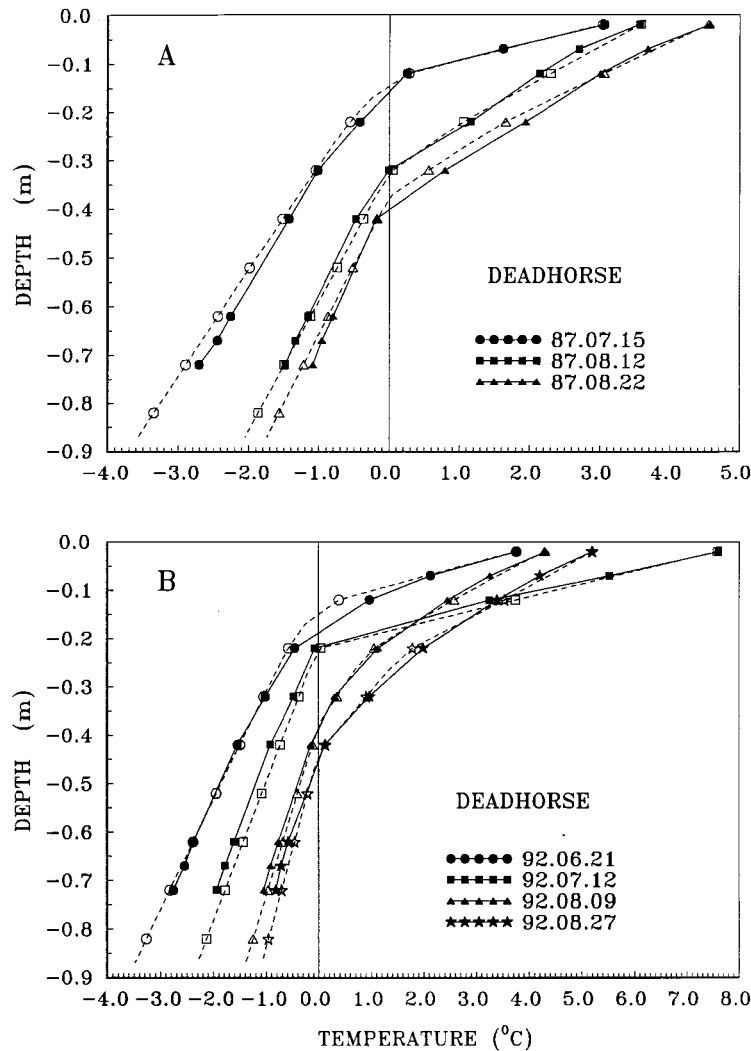


Figure 13 Calculated (dashed lines and open symbols) and measured (solid lines and filled symbols) temperature profiles at Deadhorse during the thawing period in 1987 and 1992.

provided the best fit of the numerical model to the data are shown in Table 7. Significant adjustments in the thermal conductivity were made in thawed peat for the WD and DH sites, where its values varied in the range 40–48% of the mean values, and for FB with variations of 20–27% of the mean values (Table 7). Much smaller variations were observed in the frozen peat (about 10% from the averages), and minimal variations were typical for the thawed and frozen mineral soils (about 6% for WD, no variations at DH, and about 10% for FB).

The necessity for these adjustments in the thermal conductivities is thought to be a result of interannual variations of the average water content

during the summer in the upper part of the active layer. McGaw *et al.* (1978) showed that the thermal conductivity of the active layer depends strongly on the water content using thermal conductivity measurements both *in situ* and in the laboratory. Other investigations have confirmed these results (Smirnova and Artushina, 1984; Roman and Kononov, 1984; Hinzman *et al.*, 1991). Investigations of active layer hydrology at the Toolik Lake site carried out by Hinzman *et al.* (1991) and Hinzman *et al.* (1993) show significant variations from summer to summer in the moisture content of the organic layer, while the mineral soil (silt) remained saturated with little interannual

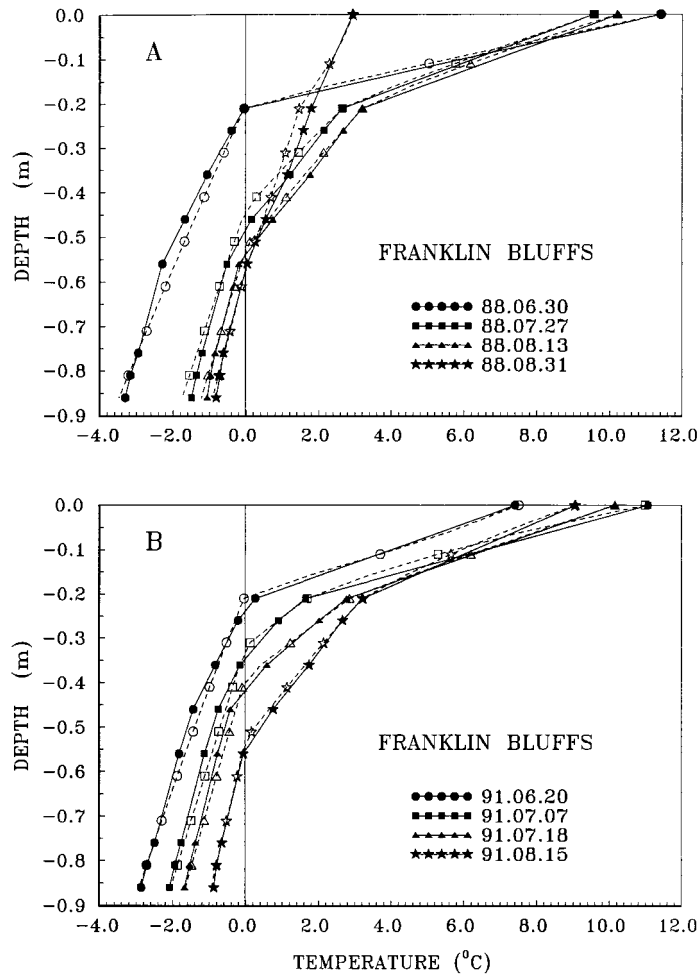


Figure 14 Calculated (dashed lines and open symbols) and measured (solid lines and filled symbols) temperature profiles at Franklin Bluffs during the thawing period in 1988 (A) and 1991 (B).

Table 7 Ratios of the thawed to frozen thermal conductivities ($\text{W m}^{-1}\text{K}^{-1}$) of the active layer estimated from the best fit of the numerical model to the data.

Soil type	1987	1988	1989	1990	1991	1992	Average
<i>West Dock</i>							
Peat I	0.7/1.4	1.0/1.7	0.6/1.5	1.0/1.7	1.3/1.4	0.7/1.4	0.88/1.52
Peat II	0.6/1.5	1.0/1.7	0.75/1.5	1.0/1.7	1.3/1.5	0.6/1.5	0.88/1.57
Silt	1.6/2.1	1.4/1.85	1.6/2.1	1.4/1.85	1.4/1.85	1.6/2.1	1.5/1.98
<i>Deadhorse</i>							
Peat I	1.3/1.5	1.2/1.3	0.8/1.5	0.8/1.3	0.8/1.3	0.7/1.5	0.93/1.4
Peat II	1.3/1.5	1.1/1.5	0.6/1.5	0.8/1.3	0.8/1.3	0.7/1.5	0.88/1.43
Silt	1.6/2.1	1.6/2.1	1.6/2.1	1.6/2.1	1.6/2.1	1.6/2.1	1.6/2.1
<i>Franklin Bluffs</i>							
Peat I	0.4/0.8	0.5/0.9	0.7/0.9	0.5/0.8	0.6/0.95	0.55/1.2	0.55/0.92
Peat II	0.5/0.9	0.5/1.0	0.5/0.9	0.5/0.9	0.6/0.95	0.6/1.2	0.54/0.98
Silt	1.15/1.5	1.35/1.7	1.15/1.5	1.15/1.5	1.4/1.7	1.3/1.8	1.25/1.62

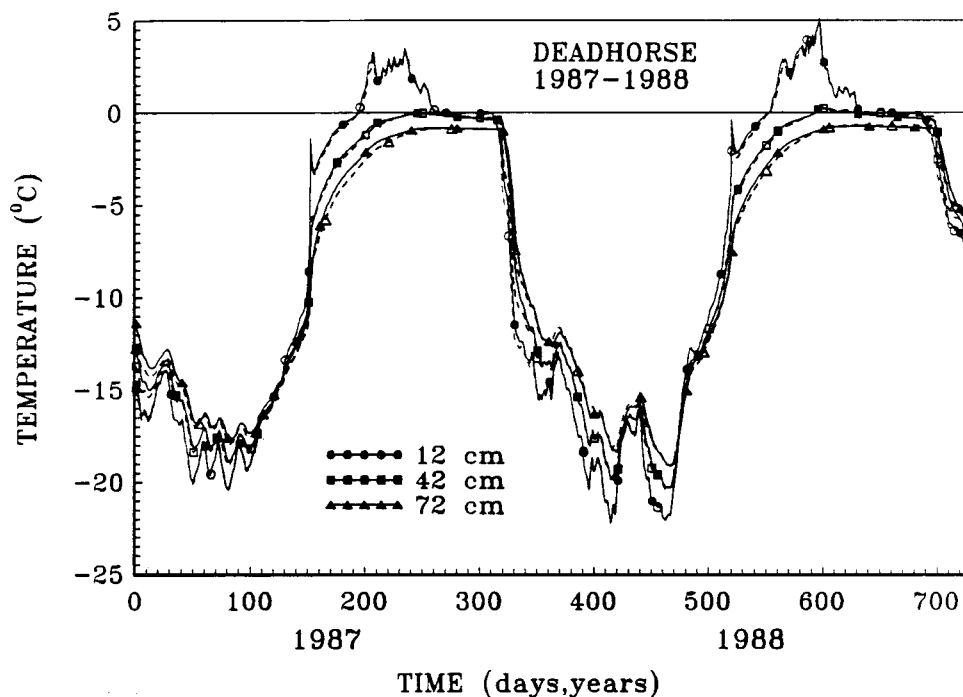


Figure 15 Comparison of calculated (dashed lines) and measured (solid lines) mean daily ground temperatures at three depths (0.12, 0.42, and 0.72 m) during 1987–88 at the Deadhorse site.

variation. Thus, the results obtained from the numerical modelling (Table 7) are consistent with the data and show that, except for the cooling period just after freeze-up, a purely conductive heat flow model can be used to accurately calculate the active layer and permafrost temperatures provided that appropriate annual adjustments are made in the thermal properties.

The adjusted values of the thermal conductivities of the active layer (Table 7) were used to recalculate maximum active layer thicknesses using the

modified Kudryavtsev equations (7)–(9) (Table 8). Comparison with the data (Table 3) shows that the average percentage difference was reduced to +2% with a range of –13% to +16%.

The adjusted values of the thermal conductivities can also be used to interpret the anomalously small values of the thermal offset, ΔT_k , defined as the difference between the mean annual permafrost surface and ground surface temperatures (Kudryavtsev *et al.*, 1974; Goodrich, 1978; Burn and Smith, 1988), found at these sites in some years

Table 8 Comparison of the calculated thicknesses of the active layer (m) using thermal conductivities from Table 7 in the modified Kudryavtsev equations (7)–(9) and measured values. Averaged thicknesses (bottom row) were calculated using input data, averaged over the whole period of measurements (1987–92).

Year	West Dock		Deadhorse		Franklin Bluffs	
	Eq. (9)	Measured	Eq. (9)	Measured	Eq. (9)	Measured
1987	0.32	0.32	0.44	0.42	0.56	0.59
1988	0.42	0.41	0.52	0.45	0.60	0.57
1989	0.48	0.46	0.70	0.69	0.72	0.72
1990	0.46	0.42	0.68	0.65	0.77	0.68
1991	0.27	0.31	0.53	0.52	0.53	0.58
1992	0.23	0.21	0.46	0.45	0.60	0.59
Mean	0.36	0.36	0.56	0.53	0.63	0.62
Averaged	0.36	0.36	0.53	0.53	0.60	0.62

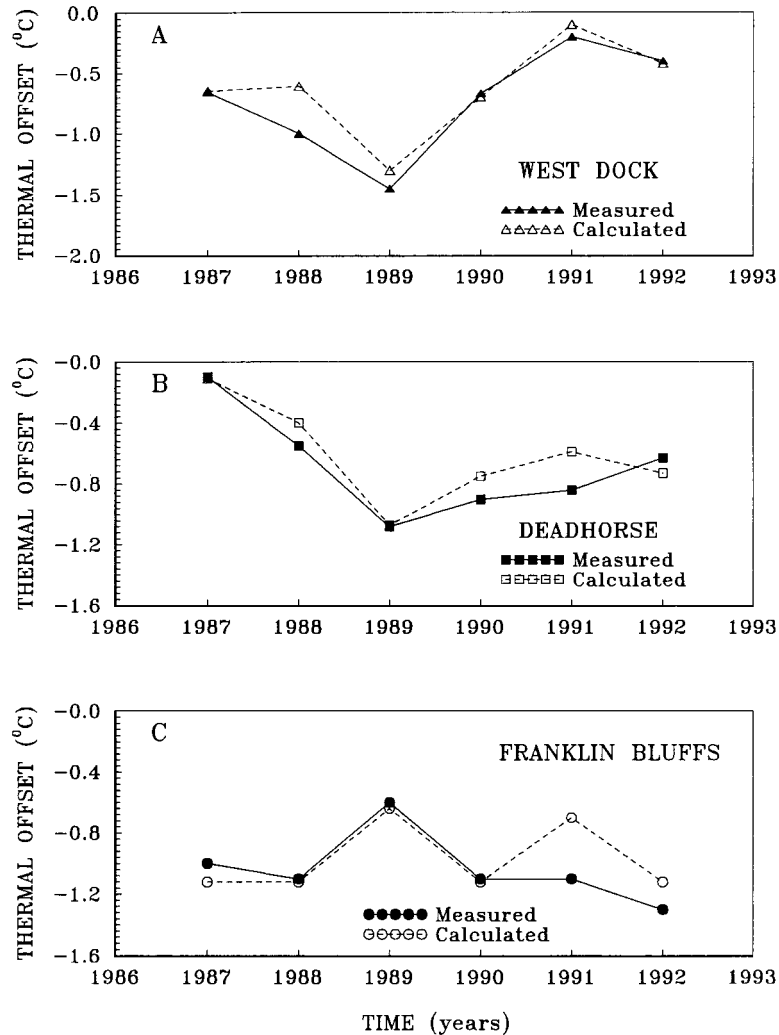


Figure 16 Comparison between measured (solid lines and filled symbols) and calculated (dashed lines and open symbols) values of thermal offset for (A) West Dock, (B) Deadhorse, and (C) Franklin Bluffs. The calculated values were obtained from equation (14) using the adjusted values of the thermal conductivities (Table 6) and thawing degree days from Romanovsky and Osterkamp (1995a).

(1991 for WD, 1987 for DH, and 1989 for FB) and which remained unexplained in a previous paper (Romanovsky and Osterkamp, 1995a). In that paper, an equation

$$\Delta T_k = \frac{I_t}{P} \left(\frac{K_t}{K_f} - 1 \right) \quad (14)$$

for calculating thermal offset was introduced. Equation (14) was derived for a homogeneous active layer with the assumption that a periodic steady state temperature regime exists at the ground surface. Figure 16 shows the correlation between interannual variations in the measured

and calculated values of the thermal offset using the adjusted values of the thermal conductivities for all three sites in (14). Values of I_t were taken from Romanovsky and Osterkamp (1995a). This figure shows significant improvement in the differences between measured and calculated values of ΔT_k from the previous paper which were generally reduced to a few tenths of a degree.

CONCLUSIONS

Air, ground surface, active layer and near-surface (to 0.7–0.9 m) permafrost temperature

measurements were made every four hours from 1986 through 1993 at three sites on a transect southward from Prudhoe Bay, Alaska together with annual temperature measurements in deeper boreholes (nominally 60 m). Using these data for validating analytical models it was shown that the modified Kudryavtsev equations (7)–(9) have several advantages compared with the classical Stefan equation (1) and the recent modification (2) introduced by Hinkel and Nicholas (1995) and can be used to make more accurate estimations of the maximum depth of seasonal thaw in the Prudhoe Bay region. The maximum average percentage difference between the measured and calculated values for Kudryavtsev's equation was -6% and the range of values was -38% to $+26\%$, while for Stefan's equation these values were $+26\%$, -3% , and $+71\%$ which shows a tendency toward overestimating thaw depths. This is thought to be caused by the assumption of no heat flow into the permafrost in the derivation of the Stefan equation. When improved data for thermal properties were used, the average difference between the measured and calculated values for Kudryavtsev's equation decreased to $+2\%$ with a range of -13% to $+16\%$.

The onset of thawing at the ground surface was closely related to snowmelt. At FB, ground thawing began about the same time or earlier than at WD and DH and usually preceded the dates for complete snowmelt at the ARCO station. For 1987–89, thawing started between 4 June and 16 June at all sites. Thawing started significantly earlier in 1990. After 1990, the thawing dates were still earlier than 1987–89 for DH and FB (between 29 May and 1 June) and approximately the same for WD (12 June in 1991 and 11 June in 1992). However, the time series of data is too short to confirm that there is a shift to earlier dates for the beginning of active layer thawing.

Although a convenient approximation of the duration of the thaw season is the number of days with positive (above 0°C) ground surface temperatures (Romanovsky and Osterkamp, 1995a), the actual time of downward movement of the thaw front was somewhat shorter. A simple analytical model (13) allowed estimates of the temperature at the ground surface when the downward movement of the thawing front (phase boundary velocity) becomes zero. These temperatures varied in the range between 1.25°C and 2.8°C for WD, between 1.4°C and 2.2°C for DH, and between 1.6°C and 2.3°C for FB, with averages of 1.75°C for WD and DH and 1.9°C for FB. At all sites, the active layer

typically reached its maximum thickness and began freezing upward from the bottom one to two weeks earlier than the beginning of freezing from the surface.

Maximum active layer thicknesses increased from the coast inland with means of 0.36 m at WD, 0.53 m at DH, and 0.62 m at FB. Active layer thicknesses were very sensitive to summer temperatures (thawing index) but were also influenced by MAGST and \bar{T}_{ps} . Active layer thicknesses have changed systematically from 1986 to the present. At WD, they changed by a factor of two (from 0.21 m to 0.45 m). Maximum thicknesses occurred at all sites in 1989 and our recent data indicate a broad minimum from 1992 until 1995. These results suggest that trace gas emissions may vary systematically if these emissions are sensitive to active layer thicknesses. Significant interannual variations of active layer thicknesses make a comparative analysis of the spatial behaviour of the active layer difficult.

The available data were used to calibrate a finite element thermal model which was then applied to simulate seasonal thawing and temperature field dynamics in the active layer and near-surface permafrost. Comparison of the results of these simulations for WD in 1987 with temperatures calculated using another numerical (finite difference) model showed 0.012 K of RMS deviation for the whole year and all depths. The deviations (RMS) between calculated (finite element model) and measured temperatures were usually in the range 0.2–0.3 K indicating that a purely conductive heat flow model can be used for accurate predictions of active layer and permafrost temperatures provided that the thermal properties are properly chosen each year. Exceptions to this occur during cooling of the active layer just after freezing and during warming of the active layer prior to thawing (Osterkamp and Romanovsky, 1997). Adjusting the thermal conductivities of the active layer to produce the smallest deviations between measured and calculated temperatures allowed estimates of the interannual variability of the thermal properties of soils. The most pronounced changes in the thermal conductivity occurred in thawed peat for the WD and DH sites, where its values varied in the range from 40% to 48% of the mean values, and for FB with variations from 20% to 27% of the mean values. Much smaller variations were observed in the frozen peat (about 10% from the averages), and minimal variations were typical for the thawed and frozen mineral soils (about 6% for WD, no variations at DH, and

about 10% for FB). These temporal variations in the thermal conductivities are thought to be a result of interannual variations of the average summer water content in the upper part of the active layer.

The adjusted values of the thermal conductivities were also used to reinterpret some anomalously small values of the thermal offset ΔT_k found at these sites in some years and which remained unexplained in a previous paper (Romanovsky and Osterkamp, 1995a). Using these adjusted values of the thermal conductivities generally reduced the differences between measured and calculated values to a few tenths of a degree.

ACKNOWLEDGEMENTS

This research was funded by the Polar Earth Sciences Program, Office of Polar Programs, National Science Foundation and by the State of Alaska. We would like to thank Dr G. Guymon, Dr L. Goodrich and Dr J. Gosink for providing the models which were used in these studies with minor modifications. We also thank numerous colleagues, graduate students, technicians and family members who helped obtain this long time series of data.

REFERENCES

- Aziz, A. and Lunardini, V. J.** (1992). Assessment of methods to predict the thickness of the active layer in permafrost regions. In *Proceedings OMAE 1992*, paper OMAE-92-209, Calgary, Canada.
- Aziz, A. and Lunardini, V. J.** (1993). Temperature variations in the active layer of permafrost. In *Proceedings of the Sixth International Conference on Permafrost*, Beijing, China. Vol. 1, pp. 17–23.
- Balobaev, V. T.** (1991). *Geothermy of the Frozen Zone of the Lithosphere, Northern Asia* (in Russian). Nauka, Novosibirsk (193 pp.).
- Barry, R. G., Armstrong, R. L., Krenke, A. N. and Kadomtseva, T. G.** (1994). *Cryospheric Indices of Global Change*. Final report, NSF grant SES-91-12420, NOAA (25 pp.).
- Burn, C. R. and Smith, C. A. S.** (1988). Observations of the 'thermal offset' in near-surface mean annual ground temperatures at several sites near Mayo, Yukon Territory, Canada. *Arctic*, **41**(2), 99–104.
- Carslaw, H. S. and Jaeger, J. C.** (1959). *Conduction of Heat in Solids*, 2nd edn. Oxford University Press, London (510 pp.).
- Goodrich, L. E.** (1976). *A Numerical Model for Assessing the Influence of Snow Cover on the Ground Thermal Regime*. PhD thesis, McGill University, Montreal (410 pp.).
- Goodrich, L. E.** (1978). Some results of a numerical study of ground thermal regimes. In *Proceedings of the Third International Conference on Permafrost*, Ottawa. National Research Council of Canada. Vol. 1, pp. 29–34.
- Gosink, J. P. and Osterkamp, T. E.** (1990). Models for permafrost thickness variation in response to changes in paleoclimate. In *Proceedings of the Fifth Canadian Permafrost Conference*, University of Laval, Quebec, Canada. pp. 191–198.
- Guymon, G. L. and Hromadka, T. V.** (1977). *Finite Element Model of Transient Heat Conduction with Isothermal Phase Change (Two and Three Dimensional)*. Corps of Engineers, US Army, CRREL Special Report 77-38, Hanover, New Hampshire (163 pp.).
- Guymon, G. L., Hromadka T. V. and Berg, R. L.** (1984). Two-dimensional model of coupled heat and moisture transport in frost-heaving soils. *Journal of Energy Resources Technology*, **106**, 336–343.
- Hinkel, K. M. and Nicholas, J. R. J.** (1995). Active layer thaw rate at a boreal forest site in Central Alaska, U.S.A. *Arctic and Alpine Research*, **27**(1), 72–80.
- Hinzman, L. D., Kane, D. L., Gieck, R. E. and Everett, K. R.** (1991). Hydrologic and thermal properties of the active layer in the Alaskan Arctic. *Cold Region Science and Technology*, **19**, 95–110.
- Hinzman, L. D., Kane, D. L. and Everett, K. R.** (1993). Hillslope hydrology in arctic setting. In *Proceedings of the Sixth International Conference on Permafrost*, Beijing, China. Vol. 1, pp. 267–271.
- Kolchugina, T. P. and Vinson, T. S.** (1993). Climate warming and the carbon cycle in the permafrost zone of the former Soviet Union. *Permafrost and Periglacial Processes*, **4**, 149–163.
- Kudryavtsev, V. A., Garagula, L. S., Kondrat'yeva, K. A. and Melamed, V. G.** (1974). *Osnovy merzlotnogo prognoza*. MGU (431 pp.). CRREL translation: V. A. Kudryavtsev et al. (1977), *Fundamentals of Frost Forecasting in Geological Engineering Investigations*. US Army CRREL draft translation 606, Hanover, NH (489 pp.).
- Lachenbruch, A. H.** (1959). Periodic heat flow in a stratified medium with application to permafrost problems. *US Geological Survey Bulletin*, 1083-A, 1–36.
- Lachenbruch, A. H. and Marshall, B. V.** (1986). Changing climate: geothermal evidence from permafrost in the Alaskan Arctic. *Science*, **234**, 689–696.
- Lachenbruch, A. H., Sass, J. H., Marshall, B. V. and Moses, T. H.** (1982). Permafrost, heat flow and the geothermal regime at Prudhoe Bay, Alaska. *Journal of Geophysical Research*, **87**(B11), 9301–9316.
- Lukyanov, V. S. and Golovko, M. D.** (1957). *Calculations of the Active Layer Thickness* (in Russian). Transgeldorfizdat, Moscow.
- McGaw, R. W., Outcalt, S. I. and Ng, E.** (1978). Thermal properties and regime of wet tundra soils at Barrow, Alaska. In *Proceedings of the Third International Conference on Permafrost*, Edmonton, Canada. Vol. 1, pp. 48–53.

- Oechel, W. C., Hastings, S. J., Vourlitis, G., Jenkins, M., Riechers, G. and Grulke, N. (1993). Recent change of Arctic tundra ecosystems from a net carbon dioxide sink to a source. *Nature*, **361**, 520–523.
- Oechel, W. C. and Vourlitis, G. L. (1994). The effect of climate change on land–atmosphere feedbacks in arctic tundra regions. *Tree*, **9**(9), 324–329.
- Osterkamp, T. E. (1985). *Temperature Measurements in Permafrost*. Report FHWA-AK-RD-85-11, Alaska DOTPF, Fairbanks, AK (87 pp.).
- Osterkamp, T. E. and Gosink, J. P. (1991). Variations in permafrost thickness in response to changes in paleoclimate. *Journal of Geophysical Research*, **94**(B3), 4423–4434.
- Osterkamp, T. E. and Romanovsky, V. E. (1996). Characteristics of changing permafrost temperatures in the Alaskan Arctic, U.S.A. *Arctic and Alpine Research*, **28**(3), 267–273.
- Osterkamp, T. E. and Romanovsky, V. E. (1997). Freeze-up of the active layer on the coastal plain in the Alaskan Arctic. *Permafrost and Periglacial Processes*, **8**, 23–44.
- Osterkamp, T. E., Zhang, T. and Romanovsky, V. E. (1994). Evidence for a cyclic variation of permafrost temperatures in northern Alaska. *Permafrost and Periglacial Processes*, **5**, 137–144.
- Pavlov, A. V. (1980). *Calculation and Regulation of the Soil Freezing Regime* (in Russian). Nauka, Novosibirsk (240 pp.).
- Porkhaev, G. V. (1970). *The Thermal Interaction between Buildings and Engineering Constructions and Permafrost* (in Russian). Nauka, Moscow (208 pp.).
- Roman, L. T. and Konovalov, A. A. (1984). Thermal properties of the peaty soils and peat. In Ershov, E. D. (ed.), *Thermal Properties of the Earth Materials* (in Russian). Moscow State University Press, Moscow, pp. 128–136.
- Romanovsky, V. E. and Osterkamp, T. E. (1994). Temporal and spatial behavior of the active layer in northern Alaska: 1986–1993, Alaska. *EOS, Transactions, American Geophysical Union*, **75**, 86 (abst.).
- Romanovsky, V. E. and Osterkamp, T. E. (1995a). Interannual variations of the thermal regime of the active layer and near-surface permafrost in Northern Alaska. *Permafrost and Periglacial Processes*, **6**(4), 313–335.
- Romanovsky, V. E. and Osterkamp, T. E. (1995b). Modeling of the permafrost temperature dynamics and active layer thawing and freezing at Prudhoe Bay, Alaska. *EOS, Transactions, American Geophysical Union*, **76**(46), 237–238 (abst.).
- Shur, Iu. L. (1988). *Upper Horizon of Permafrost and Thermokarst* (in Russian). Nauka, Novosibirsk (214 pp.).
- Smirnova, N. N. and Artushina, V. I. (1984). Thermal conductivity of soils as a function of their moisture content and density. In Ershov, E. D. (ed.), *Thermal Properties of the Earth Materials* (in Russian). Moscow State University Press, Moscow, pp. 87–93.
- Tikhonov, A. N. and Samarsky, A. A. (1966). *Mathematical Physics* (in Russian). Nauka, Moscow (367 pp.).
- Tipenko, G. S. (1987). Analytical methods to solve the heat exchange problems in geocryology. In Garagula, L. S. (ed.), *The Usage of Mathematical Methods in Geocryology* (in Russian) Moscow State University Press, Moscow, pp. 38–79.
- Zarling, J. P. (1987). Approximate solution to the Neumann problem. In *1987 International Symposium on Cold Region Heat Transfer*. American Society of Mechanical Engineering, pp. 47–57.
- Zhang, T. (1993). *Climate, Seasonal Snow Cover and Permafrost Temperatures in Alaska North of the Brooks Range*. PhD. thesis, University of Alaska, Fairbanks (232 pp.).